Hindawi Publishing Corporation
International Journal of Antennas and Propagation
Volume 2008, Article ID 254830, 8 pages
doi:10.1155/2008/254830

Research Article

Microwave Tomography for Brain Imaging: Feasibility Assessment for Stroke Detection

Serguei Y. Semenov and Douglas R. Corfield

School of Medicine, Keele University, ISTM, Hartshill Campus, Thornburrow Drive, Hartshill, Stoke-on-Trent ST4 7QB, UK

Correspondence should be addressed to Serguei Y. Semenov, s.semenov@pmed.keele.ac.uk

Received 28 September 2007; Accepted 12 March 2008

Recommended by Stuart Crozier

There is a need for a medical imaging technology, that supplements current clinical brain imaging techniques, for the near-patient and mobile assessment of cerebral vascular disease. Microwave tomography (MWT) is a novel imaging modality that has this potential. The aim of the study was to assess the feasibility, and potential performance characteristics, of MWT for brain imaging with particular focus on stroke detection. The study was conducted using MWT computer simulations and 2D head model with stroke. A nonlinear Newton reconstruction approach was used. The MWT imaging of deep brain tissues presents a significant challenge, as the brain is an object of interest that is located inside a high dielectric contrast shield, comprising the skull and CSF. However, high performance, nonlinear MWT inversion methods produced biologically meaningful images of the brain including images of stroke. It is suggested that multifrequency MWT has the potential to significantly improve imaging results.

Copyright © 2008 S. Y. Semenov and D. R. Corfield. This is an open access article distributed under the Creative Commons Attribution License, which permits unrestricted use, distribution, and reproduction in any medium, provided the original work is properly cited.

1. INTRODUCTION

A healthy brain requires an adequate blood supply. A stroke or "brain attack" compromises cerebral blood flow (CBF) leading to brain injury. This brain injury can lead to death or permanent loss of function and disability. Approximately 700 000 people, each year, will experience a stroke in the US; in 2004, stroke accounted for 1 in every 16 US deaths [1].

The brain is particularly vulnerable to disturbances in blood flow as it contains no endogenous stores of energy; it is dependent upon a continuous and sufficient level of blood flow for the constant replenishment of oxygen and glucose and for the removal of waste products. Therefore, CBF is tightly regulated to meet the brain's metabolic needs; local changes in cerebral metabolism are associated with local changes in CBF. Indeed this close coupling of metabolism and flow is the basis for functional brain imaging techniques such as $H_2{}^{15}O$ positron emission tomography (PET) and blood oxygen level dependent functional magnetic resonance imaging (FMRI). In addition to the metabolic coupling of CBF to metabolism, an intrinsic autoregulatory mechanism maintains a constant level of blood flow despite fluctuations in arterial blood pressure across a wide physiological ranges; this protects the cerebral circulation from potentially harmful changes in perfusion pressure. Thus, the normal regulation of cerebral perfusion depends on a complex interaction of metabolism, circulation, and respiration which is perturbed by pathologies such as stroke.

Acute ischemic strokes account for about 85% of all strokes; each begins with a blood clot (thrombus) forming in the circulation at a site distant from the brain. The clot breaks away from this distant site forming an embolus which then travels through the circulation; on reaching the brain, the embolus lodges in the small vessels interrupting blood flow to a portion of brain tissue. With this reduction in blood flow, tissue damage quickly ensues. Clinical management of stroke has been enhanced by the use of thrombolytics (clot busters) combined with the application of brain imaging techniques that reveal the pathophysiological changes in brain tissue that result from the stroke. In particular, the clinical decision, to use a thrombolytic, must be made within 3 hours of the onset of symptoms and requires a firm diagnosis of an ischemic stroke [2]. This clinical decision relies on imaging methods such as computed

tomography (CT) and MRI to reliably determine ischemic perfusion changes. Subsequent management of the stroke is enhanced by imaging the extent of the area of brain tissue with compromised blood flow [3]. Current clinical imaging methods, including CT, PET, and MRI each offers useful information on tissue properties related to perfusion, ischemia, and infarction [3]. Whilst each of these methods has its own advantages, none currently offers a rapid or cost effective imaging solution that can be made widely available at the "bedside" in the emergency department or to first response paramedical services. Microwave tomography (MWT) might present a safe, portable, and cost-effective supplement to current imaging modalities for acute and chronic assessment of cerebral vascular diseases including stroke.

With microwave imaging, tissues are imaged based on differences in their dielectric properties. It has been demonstrated that tissue malignancies, blood supply, hypoxia, acute ischemia, and chronic infarction [4–9] change tissue dielectric properties. Therefore, MW imaging offers the potential for the diagnosis of functional and pathological tissue conditions, including perfusion and perfusion-related injuries. MW imaging of breast malignancies has been demonstrated [8, 10–12]. Perfusion-related tissue injuries have been imaged using MWT in excised canine hearts [13] and in simulated extremities [9]. MWT of biological objects possesses very complicated problem of so-called diffraction tomography [14]. A high dielectric contrast between tissues with high water content (e.g., muscle tissue) and low water content (e.g., bone) presents an additional complication for MWT imaging. Various approaches in two-dimensional (2D) and three-dimensional (3D) geometries, using scalar and vector approximations, have been developed recently [15–25]. We have shown that experimental MWT imaging of high dielectric contrast objects is possible using nonlinear Newton and multiplicative regularised contrast source inversion (MR-CSI) methods [24]. MWT imaging of the brain presents a significant challenge, as the brain is an object of interest that is located inside a high dielectric contrast shield, comprising the skull (with low dielectric contrast ($\boldsymbol{\varepsilon}\sim$10–15) and cerebral spinal fluid (with high $\boldsymbol{\varepsilon}\sim$55–60). The aims of this project are: (i) to determine the optimal technical characteristics of an MWT brain imaging device and (ii) to assess the feasibility and potential performance characteristics of MWT for brain imaging with a particular focus on stroke detection. The methods and modeling approaches are described in Section 2; the results are presented and discussed in Section 3.

2. METHODS

The aims of the study were accomplished using computer simulations of MWT imaging of a 2D head model. The model is presented in Figure 1. The dielectric properties of the regions of normal head model, taken from published data [26–29], are summarised in Table 1. In further developing this model, to incorporate a region of acutely simulated stroke injury, we used previously obtained tissue perfusion data [4, 5, 9]. The acute stroke injury was simulated as −10

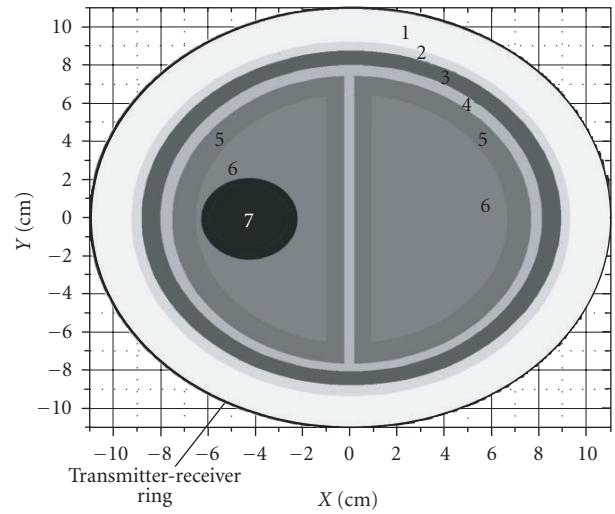

Figure 1: Simulated 2D model of a head inside of the MWT imaging chamber with a radius of 11 cm.

contrast (to white matter) circle with diameter 1, 2, or 4 cm. Further simulations were conducted using two 2D models of a head, first, with normal brain blood flow and, second, with compromised blood flow due to simulated stroke (see Figure 1).

Transmitters and receivers (positioned equidistantly) were located on the outer ring of the working chamber with a radius of 11 cm. The overall number of transmitters (N_{tr}) and receivers (N_{rec}) was 32×32 or 64×64. In general cases, the more sources/receivers that are used, the better quality of reconstructed images is expected. However, an increased number of antennas will add additional technical obstacles, such as an increase of data acquisition time, problem related to the construction of small, efficient antennas for 0.5–2.0 GHz, and so forth. See discussion following Table 3 for further details. To simulate an MWT imaging procedure, the object under the study was irradiated from jth transmitter and scattered electromagnetic (EM) field was measured on $N_{\text{rec}}/2$ opposite receivers. This was continued for each transmitter from 1 to N_{tr}. In some series of simulations, a random noise was added to received complex EM signal. The sources of EM radiation were simulated as unlimited strings over the main axis (z-axis) of the 2D model. Of course, this source model together with an overall 2D approach has limited practical application. However, the model does allow assessing the feasibility of the technology. In practical cases, we proved that a dipole model is a good approximation of ceramic loaded waveguide antennas used in our previously built systems [30–32]. The direct problem was solved on a polar grid system with uniform mesh (512 over angle $\times$256 over radius) using an approach presented elsewhere [15].

Image reconstruction was performed using the Newton approach, presented elsewhere [15]. Within this approach, we used a polar mesh with 256 (angle) $*$ 128 (radius) grids for solution of the direct problem and a Cartesian mesh with $64 * 64$ grids for inverse problem, with various regularisation parameters. Regularisation parameters were

Table 1: Dielectric properties of the head model at 1 GHz (see Figure 1).

Region Thickness	Matching solution	Skin 5 mm	Skull 7 mm	CSF 3 mm	Grey matter	White matter	Stroke area
No.	1	2	3	4	5	6	7
Dielectric properties	$40 + j13$	$40 + j11$	$13 + j2$	$57 + j26$	$50 + j18$	$40 + j15$	$36 + j13$

Table 2: Projected signal attenuation within tomographic imaging procedure of human head.

Frequency [GHz]	0.5	1.0	2.0
Attenuation [dB]	−58	−100	−156

chosen by a trial method. Two reconstruction schemes were used: single frequency and multi (dual)-frequencies. Within single frequency schemes, the image reconstruction was started with a homogeneous background medium of matching solution, therefore, no a priori information taken into account. Within the multifrequency schemes there was a sequential chain of reconstructions at each frequency. An initial reconstruction was started from a homogeneous background medium using scattered EM fields obtained at the 1st frequency, while, at the sequential step(s) we used different frequencies (with corresponding scattered EM fields obtained at that frequencies) and started from the results of reconstruction obtained at previous step(s). This procedure was performed using different frequencies from 0.5 GHz to 2.0 GHz At this stage, the frequency dispersion of dielectric properties of the various tissues was not taken into account. The potential impact of this assumption is discussed in the next section.

3. RESULTS AND DISCUSSION

The technical performance of MWT brain imaging approach was initially assessed over a frequency range from 0.5 GHz to 2.5 GHz using the model and direct problem solver. The ultimate goal is to develop microwave tomographic technology with the best sensitivity and specificity, and with high temporal and spatial resolution, for the noninvasive assessment of brain tissues. The best spatial resolution can be achieved at high frequencies. However, the attenuation of EM radiation in biological media is in inverse ratio with the frequency, with decreasing signal-to-noise ratio (SNR) at high frequencies. Therefore, the strategy is to find the highest possible frequency at which receivers will still be able to detect signal with reliable SNR and will not compromise temporal resolution. Using our MWT simulation approach, together with the model of the head (see Figure 1), we estimated an overall signal attenuation summarised in Table 2. The results should be taken as a guidance or initial estimation, which does not take into account dispersion of tissue dielectric properties, any particulars of head geometry, and so forth.

As can be seen, the attenuation is very high at frequencies above 1 GHz-2 GHz range. As it is highly desirable: (i) to achieve a good SNR ratio (within a range of 40–60 dB) for biological detection reasons, such as sensitivity, specificity, and resolution and (ii) to not increase data acquisition time for measuring highly attenuated signals, which compromises an expected very attractive time resolution (within msec range) in order to detect circulated gated tissue changes, we suggest that frequencies within 0.5 to 1.0 GHz might be an optimal for brain imaging. An additional expected advantage, of using this low portion of microwave spectrum, is that acute perfusion related changes in tissue dielectric properties are more pronounced at low frequencies [4, 5]. This choice might unfavorably affect spatial resolution in its classical, far-EM-field sense. However, there is potential to improve spatial resolution, even to obtain a super-resolution in near-EM-field using nonlinear inversion [33, 34].

We further assessed the potential resolution of the technology to detect acute "stroke-like" areas with −10% contrast in dielectric properties. It has to be noted here that this is different from the classical spatial resolution definition, which is defined as a minimal distance (using Raleigh or half-height criteria) at which two small similar inhomogeneities can be distinguished between each other. Previously, we conducted such studies and experimentally achieved a 7–9 mm spatial resolution at 0.9 GHz [35]. In this study, the aim was to understand what was the smallest size of brain inhomogeneity, with a particular dielectric contrast, that could potentially be detected. In our previous MWT imaging studies, we suggested that changes in about 1% in amplitude and about 1 degree in phase of the received EM signal could be confidently detected and corresponding alterations in dielectric properties could be successfully reconstructed. We simulated MWT data acquisition for brain models with and without stroke areas of different size and then averaged differences in received EM signals over all receivers for each of transmitter position. The averaged differences in EM signals at 1 GHz for normal brain, and brain with stroke, were about: 3.8% in amplitude and 5.5° in phase for 4 cm diameter stroke, 1.2% and 2° for 2 cm and 0.3% and 0.2° for 1 cm correspondingly. Therefore, it is suggested that, at this level of the development of MWT imaging technology, the smallest imaginable area of acute stroke is estimated to be about 2 cm in diameter. This resolution might not compare with the one achieved by other imaging modalities, such as MRI or CT. However, all performance factors should be considered together. Excellent temporal resolution will add a novel diagnostic dimension. Cost efficiency, mobility, and safety are other significant factors which suggest potential advantages of MWT for brain imaging.

An MWT imaging cycle was simulated as described in the method section. The results of the first series of

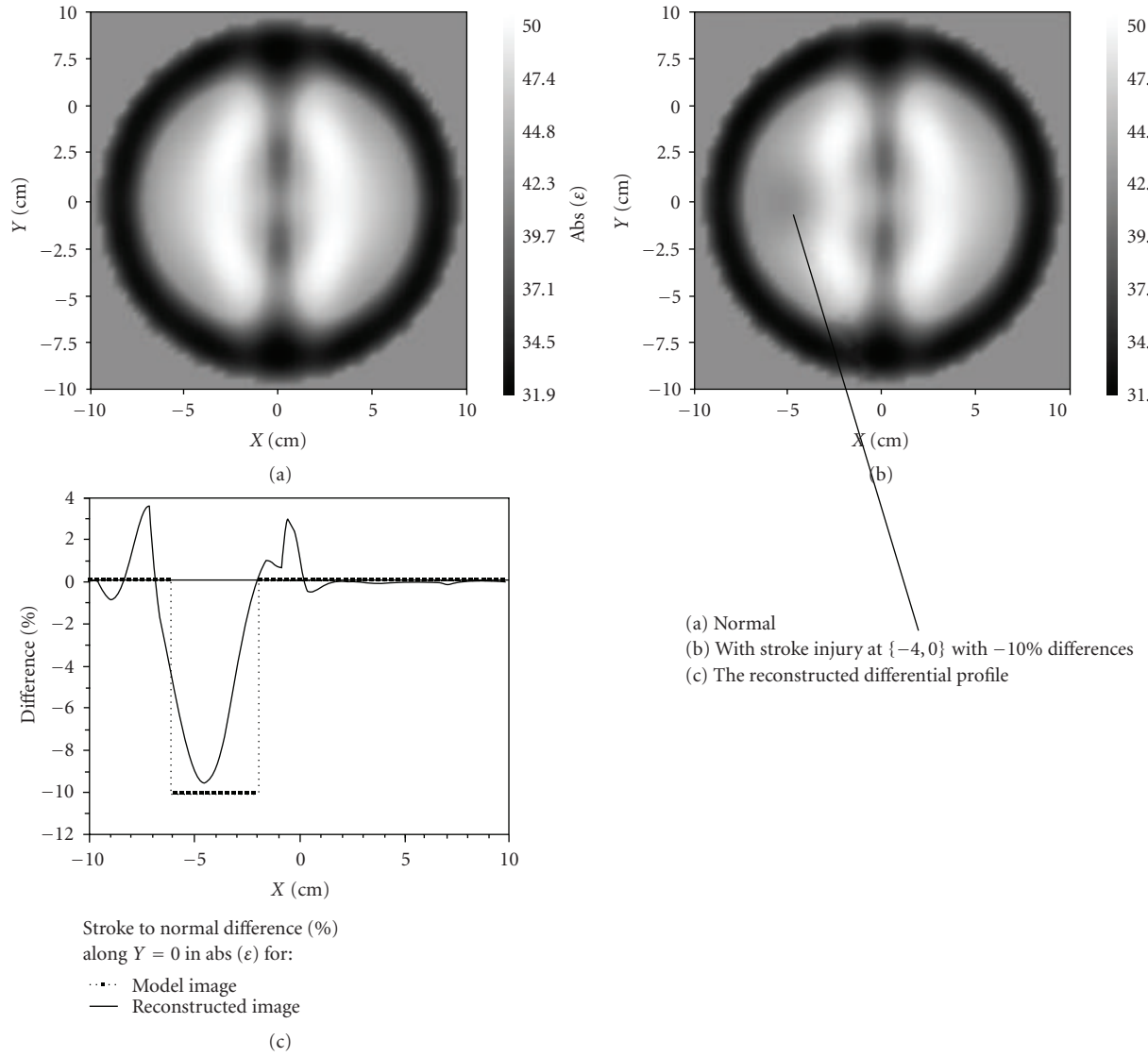

Figure 2: Reconstructed MWT images of simulated brain model: (a) normal and (b) with a stroke injury with radius 2 cm centered at $\{-4, 0\}$, (c) the reconstructed differential profile [% difference] through the stroke area. Noiseless case. Frequency 1 GHz.

imaging experiments are presented in Figure 2 for 1 GHz frequency for the 32×32 transmitters $\times$ receivers case. The absolute values of the reconstructed dielectric properties of (a) the normal brain image can be compared with (b) those reconstructed properties for the stroke case. The reconstructed profile through the stroke area of a radius 2 cm located at $X = -4$ cm and $Y = 0$ cm is presented in (c) as % difference in reconstructed values between normal and stroke cases. The shadow of the stroke area can be easy appreciated from the reconstructed image (b). Furthermore, the reconstructed differential profile (c) clearly indicates an area of dielectric inhomogeneity (stroke) in terms of both the geometrical position and the absolute values of the reconstructed dielectric properties, as evidenced by the proximity of the reconstructed profile (line in c) to the expected simulated profile (dots in c).

Next, we focused on the MWT imaging performance at different frequencies with 1% noise. This noise figure does require a good performance of both MWT imaging hardware and the overall MWT imaging reconstruction protocol but is achievable in practice. We used the brain model, with the stroke area of a radius 2 cm located at $\{-4; 0\}$. The imaging results are presented in Figure 3 for frequencies (a) 0.5 GHz, (b) 1.0 GHz, and (c) 2.0 GHz. The area with suspected stroke injury is circled in white. The stroke injury area failed to be reconstructed when a high frequency (2 GHz) is used alone. This unsuccessful imaging result might be attributed to (i) a very high attenuation of EM field at this frequency (see Table 2) and/or to (ii) weaknesses of used imaging approach. However, the used imaging algorithm based on the Newton approach has previously shown a good imaging performance, which is comparable with other powerful,

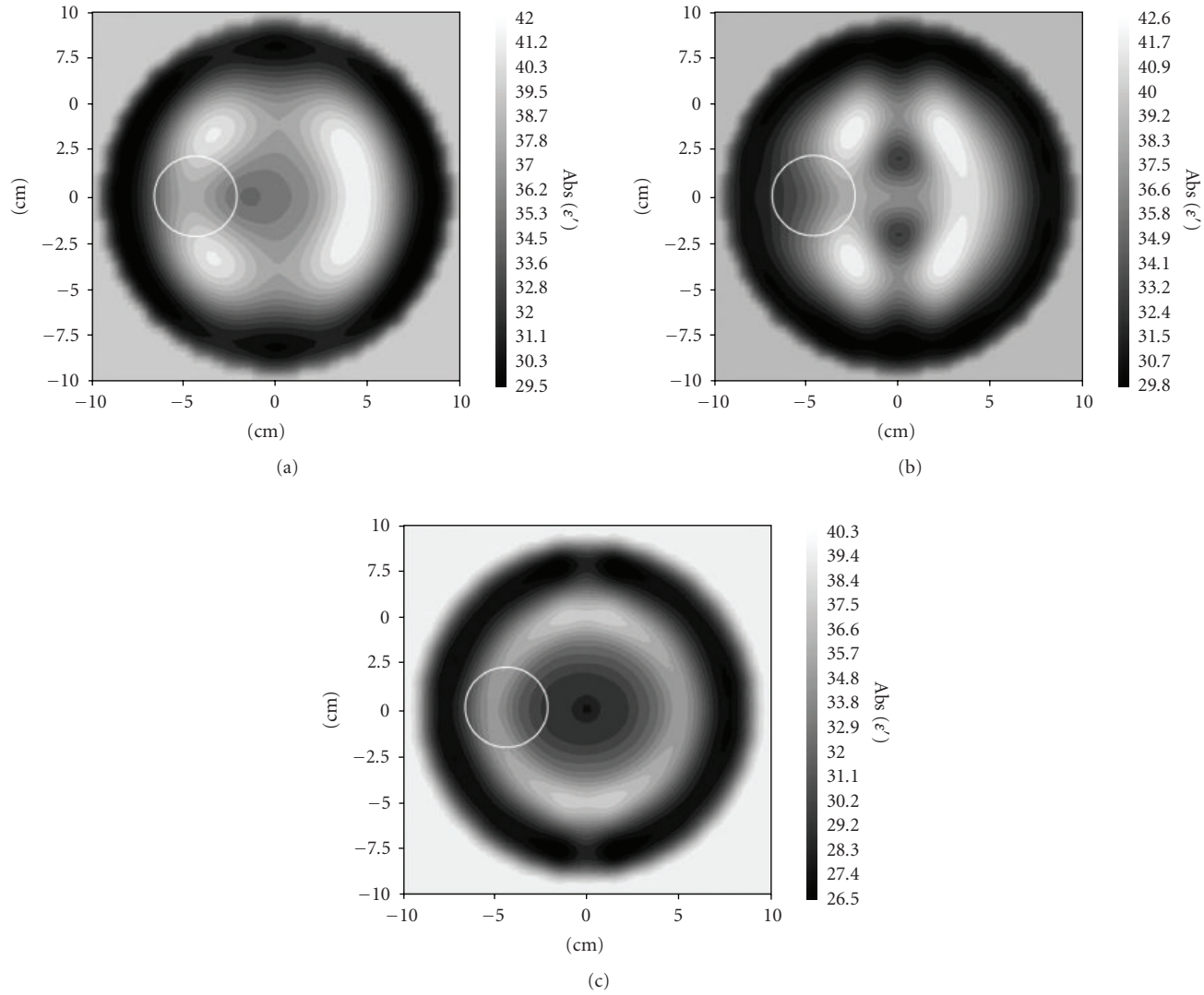

Figure 3: Reconstructed MWT images of simulated brain model with a stroke injury with radius 2 cm located at $\{-4, 0\}$ obtained at frequencies (a) 0.5 GHz, (b) 1.0 GHz, and (c) 2.0 GHz. 1% noise. Area with suspected stroke injury is circled in white.

recently developed nonlinear methods of MWT, such as gradient method and contrast source inversion method [15, 24]. An area of stroke injury was reconstructed when MWT imaging was performed at lower frequencies (0.5–1.0 GHz), with more pronouncing detection at 1 GHz (b).

A multifrequency approach further improved the imaging results. Images, obtained at 0.5 GHz and 2.0 GHz, were used as a starting point (initial guess) for further data inversion at 1 GHz. Corresponding scattered EM fields, obtained at individual frequencies, were used. At this stage, the frequency dispersion of dielectric properties of various tissues was not taken into account, that is, we used the same dielectric parameters of the model at 0.5 GHz and 2.0 GHz as we did at 1 GHz (see Table 1). The dielectric properties of biological tissues at this frequency band show significant dispersion. For example, for an averaged brain tissue they vary from $48.5 + j22.7$ at 0.5 GHz to $43.2 + j11.8$ at 2.0 GHz [29]. These variations can be incorporated into a multifrequency reconstruction approach later on, using well-developed models of tissue dielectric properties, such as the Cole-Cole model or the multicomponent Schwan approach. The aim here was to assess if multifrequency MWT imaging has the potential to improve brain imaging. This is demonstrated in Figure 4, when two multifrequency approaches were used. The first one (a) uses an initial imaging procedure at 0.5 GHz continuing at 1 GHz; the second one uses an initial inversion at 2.0 GHz continuing at 1 GHz. Both approaches demonstrate significant image improvement as compared with the 1st phase of reconstruction (see Figure 3). The area of stroke injury (circled in white) has been reconstructed using both approaches. There is room for improvement and optimisation of multifrequency MWT imaging, which should be a focus of further simulation and experimental studies. The most interesting and technically important question, at the moment, is how distant should frequencies be? If the frequency gap can be narrowed, then

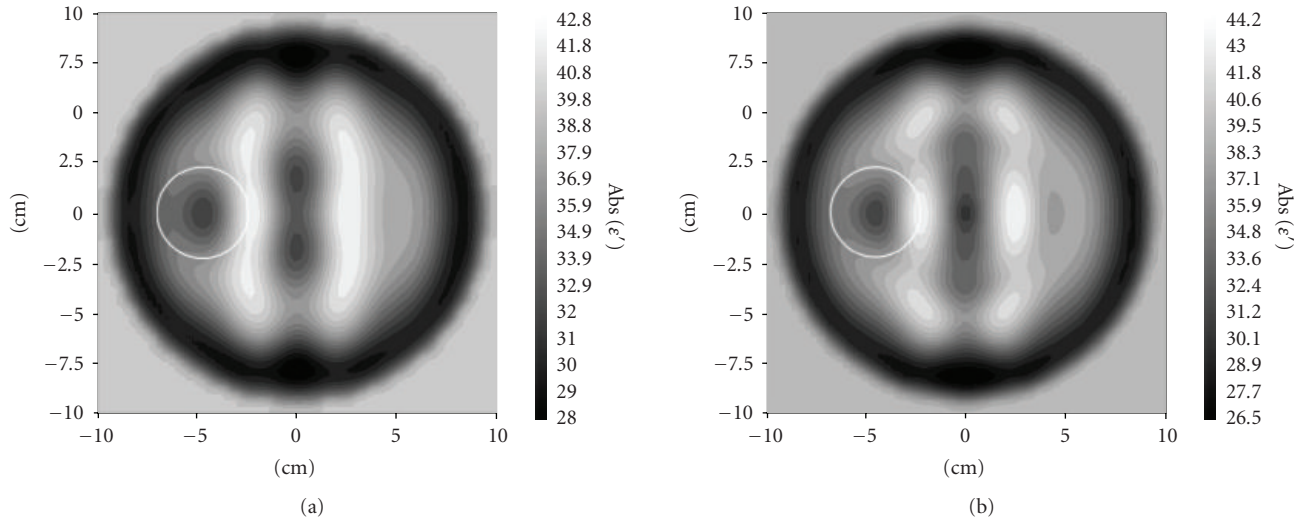

Figure 4: Reconstructed MWT images of simulated brain model with a stroke injury with radius 2 cm located at $\{-4, 0\}$ obtained using multifrequency reconstruction: (a) 0.5 GHz and 1.0 GHz and (b) 2.0 GHz and 1.0 GHz. 1% noise. Area with suspected stroke injury is white circled.

Table 3: Characteristics and projected performance of an initial MWT system for brain imaging.

MW frequencies	0.7–1.0 GHz
Imaging chamber	3D "Helmet" like, with R~11 cm
Number of antennas per a 2D "slice" of an imaging chamber	32–64
Type of antennas	ceramic ($\boldsymbol{\varepsilon}$~60–90) loaded waveguides
Each antenna works as transmitter and receiver	Yes
Measured attenuations [dB]	60–110
S/N ratio [dB]	40–60
IFBW [kHz]	1–10
Output power on antenna	+20 dBm

(i) tissue dispersion might not be taken into account and (ii) narrow band efficient antennas may be used instead of wide band, or a family of narrow bands, antennas.

Presented imaging results are not perfect. However, they indicate that MWT has the potential to determine perfusion related changes in the human brain and that MWT could be developed as a useful new imaging modality for stroke management. There is room for further images improvement at both stages: during reconstruction and at post-processing afterwards.

The projected characteristics of an initial practical MWT system for brain imaging are summarised in Table 3. We intend to use ceramic loaded (with $\boldsymbol{\varepsilon}$~60–90) waveguide antennas as previously successfully used EM sources within MWT imaging chamber [30–32]. The typical dimensions of the antenna tip facing the imaging chamber for frequency of interest are 21 mm × 7 mm. This gives a maximal number of antennas per a 2D "slice" of an imaging chamber of about 32 to 90, depending on an antenna rotation and, consequentially, an imaging approach used (2D, 3D scalar or 3D vector).

4. CONCLUSIONS

(1) The MWT imaging of deep brain tissues and stroke detection presents a significant challenge, being an object of interest located inside of a high dielectric contrast shield, comprising the skull and cerebral spinal fluid.

(2) High performance, nonlinear MWT inversion methods were able to produce biologically meaningful images including images of stroke. At this level of the development of MWT imaging technology, the smallest imaginable area of acute stroke is estimated to be about 2 cm.

(3) Suggested multifrequency MWT has potentials for significant improvement of imaging results.

REFERENCES

[1] W. Rosamond, K. Flegal, G. Friday, et al., "Heart disease and stroke statistics—2007 update: a report from the American Heart Association Statistics Committee and Stroke Statistics Subcommittee," *Circulation*, vol. 115, no. 5, pp. e69–e171, 2007.

[2] H. P. Adams Jr., G. del Zoppo, M. J. Alberts, et al., "Guidelines for the early management of adults with ischemic stroke," *Stroke*, vol. 38, no. 5, pp. 1655–1711, 2007.

[3] K. W. Muir, A. Buchan, R. von Kummer, J. Rother, and J.-C. Baron, "Imaging of acute stroke," *Lancet Neurology*, vol. 5, no. 9, pp. 755–768, 2006.

[4] S. Y. Semenov, R. H. Svenson, and G. P. Tatsis, "Microwave spectroscopy of myocardial ischemia and infarction. 1. Experimental study," *Annals of Biomedical Engineering*, vol. 28, no. 1, pp. 48–54, 2000.

[5] S. Y. Semenov, R. H. Svenson, V. G. Posukh, et al., "Dielectrical spectroscopy of canine myocardium during acute ischemia and hypoxia at frequency spectrum from 100 kHz to 6 GHz," *IEEE Transactions on Medical Imaging*, vol. 21, no. 6, pp. 703–707, 2002.

[6] W. T. Joines, Y. Zhang, C. Li, and R. L. Jirtle, "The measured electrical properties of normal and malignant human tissues from 50 to 900 MHz," *Medical Physics*, vol. 21, no. 4, pp. 547–550, 1994.

[7] A. J. Surowiec, S. S. Stuchly, J. R. Barr, and A. Swarup, "Dielectric properties of breast carcinoma and the surrounding tissues," *IEEE Transactions on Biomedical Engineering*, vol. 35, no. 4, pp. 257–263, 1988.

[8] E. C. Fear, S. C. Hagness, P. M. Meaney, M. Okoniewski, and M. A. Stuchly, "Enhancing breast tumor detection with near-field imaging," *IEEE Microwave Magazine*, vol. 3, no. 1, pp. 48–56, 2002.

[9] S. Y. Semenov, J. Kellam, P. Althausen, et al., "Microwave tomography for functional imaging of extremity soft tissues: feasibility assessment," *Physics in Medicine and Biology*, vol. 52, no. 18, pp. 5705–5719, 2007.

[10] P. M. Meaney, M. W. Fanning, D. Li, S. P. Poplack, and K. D. Paulsen, "A clinical prototype for active microwave imaging of the breast," *IEEE Transactions on Microwave Theory and Techniques*, vol. 48, no. 11, pp. 1841–1853, 2000.

[11] E. C. Fear and M. A. Stuchly, "Microwave detection of breast cancer," *IEEE Transactions on Microwave Theory and Techniques*, vol. 48, no. 11, pp. 1854–1863, 2000.

[12] S. C. Hagness, A. Taflove, and J. E. Bridges, "Three-dimensional FDTD analysis of a pulsed microwave confocal system for breast cancer detection: design of an antenna-array element," *IEEE Transactions on Antennas and Propagation*, vol. 47, no. 5, pp. 783–791, 1999.

[13] S. Y. Semenov, A. E. Bulyshev, V. G. Posukh, Y. E. Sizov, T. C. Williams, and A. E. Souvorov, "Microwave tomography for detection/imaging of myocardial infarction. I. Excised canine hearts," *Annals of Biomedical Engineering*, vol. 31, no. 3, pp. 262–270, 2003.

[14] A. J. Devaney, "Current research topics in diffraction tomography," in *Inverse Problmes in Scattering and Imaging*, M. Bertero and E. R. Pike, Eds., pp. 47–58, Adam Hilger, New York, NY, USA, 1992.

[15] A. E. Souvorov, A. E. Bulyshev, S. Y. Semenov, et al., "Microwave tomography: a two-dimensional Newton iterative scheme," *IEEE Transactions on Microwave Theory and Techniques*, vol. 46, no. 11, pp. 1654–1659, 1998.

[16] R. E. Kleinman and P. M. van den Berg, "Modified gradient method for two-dimensional problems in tomography," *Journal of Computational and Applied Mathematics*, vol. 42, no. 1, pp. 17–35, 1992.

[17] A. E. Bulyshev, A. E. Souvorov, S. Y. Semenov, et al., "Three-dimensional microwave tomography. Theory and computer experiments in scalar approximation," *Inverse Problems*, vol. 16, no. 3, pp. 863–875, 2000.

[18] A. Abubakar, P. M. van den Berg, and J. J. Mallorqui, "Imaging of biomedical data using a multiplicative regularized contrast source inversion method," *IEEE Transactions on Microwave Theory and Techniques*, vol. 50, no. 7, pp. 1761–1771, 2002.

[19] N. Joachimowicz, J. J. Mallorqui, J.-C. Bolomey, and A. Broquetas, "Convergence and stability assessment of Newton-Kantorovich reconstruction algorithms for microwave tomography," *IEEE Transactions on Medical Imaging*, vol. 17, no. 4, pp. 562–570, 1998.

[20] P. Lobel, R. E. Kleinman, Ch. Pichot, L. Blanc-Féraud, and M. Borlaud, "Conjugate-gradient method for solving inverse scattering with experimental data," *IEEE Antennas and Propagation Magazine*, vol. 38, no. 3, pp. 48–51, 1996.

[21] W. C. Chew and Y. M. Wang, "Reconstruction of two-dimensional permittivity distribution using the distorted Born iterative method," *IEEE Transactions on Medical Imaging*, vol. 9, no. 2, pp. 218–225, 1990.

[22] H. Harada, D. J. N. Wall, T. Takenaka, and M. Tanaka, "Conjugate gradient method applied to inverse scattering problem," *IEEE Transactions on Antennas and Propagation*, vol. 43, no. 8, pp. 784–792, 1995.

[23] P. M. Meaney, K. D. Paulsen, A. Hartov, and R. K. Crane, "Microwave imaging for tissue assessment: initial evaluation in multitarget tissue-equivalent phantoms," *IEEE Transactions on Biomedical Engineering*, vol. 43, no. 9, pp. 878–890, 1996.

[24] S. Y. Semenov, A. E. Bulyshev, A. Abubakar, et al., "Microwave-tomographic imaging of the high dielectric-contrast objects using different image-reconstruction approaches," *IEEE Transactions on Microwave Theory and Techniques*, vol. 53, no. 7, pp. 2284–2293, 2005.

[25] A. E. Bulyshev, A. E. Souvorov, S. Y. Semenov, V. G. Posukh, and Y. E. Sizov, "Three-dimensional vector microwave tomography: theory and computational experiments," *Inverse Problems*, vol. 20, no. 4, pp. 1239–1259, 2004.

[26] A. Peyman, S. J. Holden, S. Watts, R. Perrott, and C. Gabriel, "Dielectric properties of porcine cerebrospinal tissues at microwave frequencies: in vivo, in vitro and systematic variation with age," *Physics in Medicine and Biology*, vol. 52, no. 8, pp. 2229–2245, 2007.

[27] S. Gabriel, R. W. Lau, and C. Gabriel, "The dielectric properties of biological tissues: II. Measurements in the frequency range 10 Hz to 20 GHz," *Physics in Medicine and Biology*, vol. 41, no. 11, pp. 2251–2269, 1996.

[28] G. Schmid, G. Neubauer, and P. R. Mazal, "Dielectric properties of human brain tissue measured less than 10 h postmortem at frequencies from 800 to 2450 MHz," *Bioelectromagnetics*, vol. 24, no. 6, pp. 423–430, 2003.

[29] C. Gabriel, "Compilation of the dielectric properties of body tissues at RF and microwave frequencies," Tech. Rep. AL/OE-TR-1996-0037, Brooks Air Force Base, San Antonio, Tex, USA, 1996, http://www.fcc.gov/fcc-bin/dielec.sh.

[30] S. Y. Semenov, R. H. Svenson, A. E. Boulyshev, et al., "Microwave tomography: two-dimensional system for biological imaging," *IEEE Transactions on Biomedical Engineering*, vol. 43, no. 9, pp. 869–877, 1996.

[31] S. Y. Semenov, R. H. Svenson, A. E. Bulyshev, et al., "Three-dimensional microwave tomography: experimental prototype of the system and vector Born reconstruction method," *IEEE Transactions on Biomedical Engineering*, vol. 46, no. 8, pp. 937–946, 1999.

[32] S. Y. Semenov, R. H. Svenson, A. E. Bulyshev, et al., "Three-dimensional microwave tomography: initial experimental imaging of animals," *IEEE Transactions on Biomedical Engineering*, vol. 49, no. 1, pp. 55–63, 2002.

[33] P. M. Meaney, K. D. Paulsen, A. Hartov, and R. K. Crane, "Microwave imaging for tissue assessment: initial evaluation in multitarget tissue-equivalent phantoms," *IEEE Transactions on Biomedical Engineering*, vol. 43, no. 9, pp. 878–890, 1996.

[34] F.-C. Chen and W. C. Chew, "Experimental verification of super resolution in nonlinear inverse scattering," *Applied Physics Letters*, vol. 72, no. 23, pp. 3080–3082, 1998.

[35] S. Y. Semenov, R. H. Svenson, A. E. Bulyshev, et al., "Spatial resolution of microwave tomography for detection of myocardial ischemia and infarction-experimental study on two-dimensional models," *IEEE Transactions on Microwave Theory and Techniques*, vol. 48, no. 4, pp. 538–544, 2000.

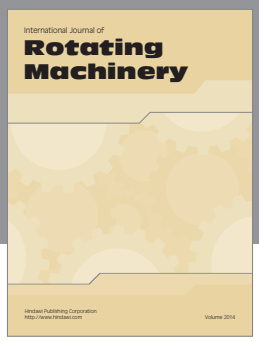

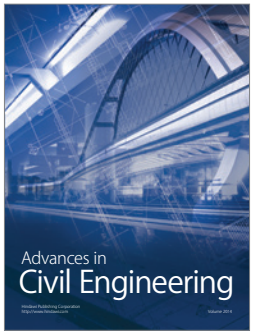

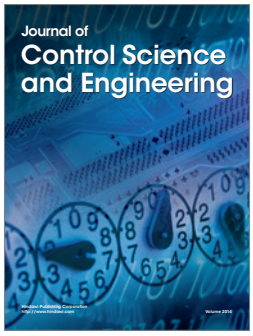

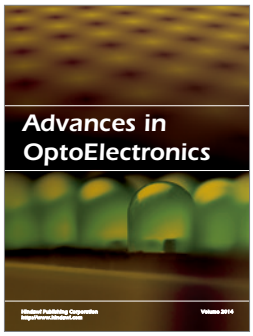

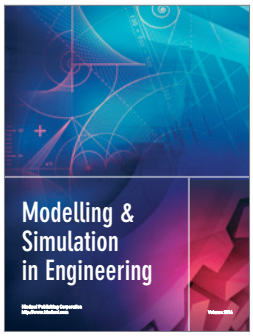

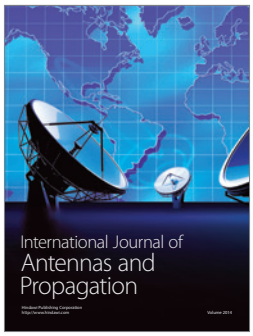

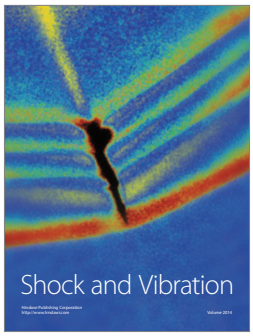

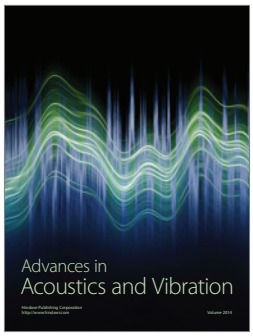

Hindawi

Submit your manuscripts at
http://www.hindawi.com